

This article was published in Environmental Science and Pollution Research, 21, 1292-12303., 2014
<http://dx.doi.org/10.1007/s11356-013-2014-1>

Assessment of solar driven TiO₂-assisted photocatalysis efficiency on amoxicillin degradation

João H. O. S. Pereira & Ana C. Reis & Olga C. Nunes & Maria T. Borges & Vítor J. P. Vilar & Rui A. R. Boaventura

J. H. O. S. Pereira · V. J. P. Vilar (✉) · R. A. R. Boaventura Laboratory of Separation and Reaction Engineering (LSRE), Associate Laboratory LSRE/LCM, Departamento de Engenharia Química, Faculdade de Engenharia da Universidade do Porto, Rua Dr. Roberto Frias, 4200-465 Porto, Portugal e-mail: vilar@fe.up.pt

A. C. Reis · O. C. Nunes

Laboratory of Process, Environmental and Energy Engineering (LEPAE), Departamento de Engenharia Química, Faculdade de Engenharia da Universidade do Porto, Rua Dr. Roberto Frias, 4200-465 Porto, Portugal

M. T. Borges

Centre for Marine and Environmental Research (CIMAR), Departamento de Biologia, Faculdade de Ciências da Universidade do Porto, Rua Campo Alegre, 4169-007 Porto, Portugal

Abstract

The objective of this work was to evaluate the efficiency of a solar TiO₂-assisted photocatalytic process on amoxicillin (AMX) degradation, an antibiotic widely used in human and veterinary medicine. Firstly, solar photolysis of AMX was compared with solar photocatalysis in a compound parabolic collectors pilot scale photoreactor to assess the amount of accumulated UV energy in the system (Q_{UV})

necessary to remove 20 mg L⁻¹ AMX from aqueous solution and mineralize the intermediary by-products. Another experiment was also carried out to accurately follow the antibacterial activity against *Escherichia coli* DSM 1103 and *Staphylococcus aureus* DSM 1104 and mineralization of AMX by tracing the contents of dissolved organic carbon (DOC), low molecular weight carboxylate anions, and inorganic anions. Finally, the influence of individual inorganic ions on AMX photocatalytic degradation efficiency and the involvement of some reactive oxygen species were also

assessed. Photolysis was shown to be completely ineffective, while only 3.1 kJUVL⁻¹ was sufficient to fully degrade 20 mg L⁻¹ AMX and remove 61 % of initial DOC content in the presence of the photocatalyst and sunlight. In the experiment with an initial AMX concentration of

40 mg L⁻¹, antibacterial activity of the solution was considerably reduced after elimination of AMX to levels below the respective detection limit. After 11.7 kJUVL⁻¹, DOC decreased by 71 %; 30 % of the AMX nitrogen was converted into ammonium and all sulfur compounds were converted into sulfate. A large percentage of the remaining DOC was in the form of low molecular weight carboxylic acids. Presence of phosphate ions promoted the removal of AMX from solution, while no sizeable effects on the kinetics were found for other inorganic ions. Although the AMX degradation was mainly attributed to hydroxyl radicals, singlet oxygen also plays an important role in AMX self-photosensitization under UV/ visible solar light.

Introduction

The most widely used group of antibiotics in human medicine in Europe is the penicillins, which have showed an increasing trend of prescription over the last decade (Versporten et al. 2011). In 2009, they represented 47 % of total outpatient use, from which the use of amoxicillin (AMX) alone, or combined with β -lactamase inhibitors, represented 83.9 % (Versporten et al. 2011). The combination of this high level of prescription and the fact that amoxicillin has a low metabolic rate in humans, leading to excretion rates of 80–90 % (Hirsch et al. 1999), accounts for an ubiquitous presence of this pharmaceutical in domestic and hospital wastewaters (Andreozzi et al. 2004; Långin et al. 2009; Watkinson et al. 2009; Leung et al. 2012). Adding to the varying efficiencies reported for the removal of antibiotics in conventional wastewater treatment plants (WWTP), which were not specifically designed to remove them (Leung et al. 2012), amoxicillin, as well as other antibacterial drugs, are frequently found in rivers and other water bodies receiving treated WWTP effluents (Kasprzyk-Hordern et al. 2008). Another source of antibiotic contamination may result from animal husbandry use as is the case of fish farming activities (Lalumera et al. 2004; Rigos and Troisi 2005), where effluents resulting from bath immersion treatments using amoxicillin concentrations as high as 200 mg L⁻¹ (Mitchell and Rodger 2011) require special consideration before disposal. These are often diluted in aquatic receiving bodies or often treated with nondestructive methods (Noga 2010). Despite the fact that some of these substances do not persist due to natural degradation processes (Jones et al. 2005), their continual release to the environment raises several concerns regarding their ecotoxicological potential to humans and animals (Kim and Aga 2007; Martinez 2009; Santos et al. 2010; Escher et al. 2011).

Several alternative treatments have been proposed in recent years to tackle this situation, which are summarized in the revision performed by Homem and Santos (2011) and Michael et al. (2013). Among them, advanced oxidation processes (AOPs) comprise different processes of generating hydroxyl radicals (\cdot OH), which are very reactive and not highly selective. AOPs can be divided in photochemical (UV, UV/O₃, and UV/H₂O₂), photocatalytic (TiO₂/UV, and Fe²⁺/H₂O₂/UV-vis) or chemical oxidation processes (O₃, O₃/H₂O₂, and H₂O₂/Fe²⁺; Poyatos et al. 2009). Their operation for full chemical degradation can be rather costly, so research is being focused on the application of AOPs that rely on solar irradiation as the source of UV radiation

(such as heterogeneous photocatalysis and photo-Fenton reaction) and the possible combination with a pre or post biological treatment step (Malato et al. 2009; Oller et al. 2011).

Although several bench-scale studies on different AOPs using simulated UV radiation applied to aqueous solutions of amoxicillin have been undertaken (Elmolla and Chaudhuri 2009; Rizzo et al. 2009; Elmolla and Chaudhuri 2010a, b, c, 2011; Dimitrakopoulou et al. 2012), only three report results from solar photo-Fenton (Trovó et al. 2008; Mavronikola et al. 2009) and solar TiO₂ (Klauson et al. 2010) processes. However, to the best of our knowledge, none so far have neither applied compound parabolic collectors (CPC) as photoreactors, nor have studied the influence of the individual presence of common occurring inorganic ions on the degradation of amoxicillin in aqueous solution. Theoretical and experimental studies (Fernández et al. 2005; González et al. 2009; Vilar et al. 2009; Colina-Márquez et al. 2010) have shown that CPCs are highly efficient on collecting solar radiation, so they are considered the best choice for different solar photocatalytic processes (Malato et al. 2002).

Thus, the main objective of this work was to study the enhancement of the photocatalytic degradation of AMX in a CPC pilot plant, promoted by the presence of suspended TiO₂ and natural sunlight, when compared with solar photolysis. AMX mineralization was assessed in terms of dissolved organic carbon (DOC), low molecular weight carboxylate ions, and inorganic ions present in the solution. The antibacterial activity was assessed at different phototreatment times and correlated with the AMX concentration. A figure-of-merit, collector area per order (ACO), was employed for both photocatalytic experiments in order to assess the possible factors that may affect the facility's efficiency, such as average solar UV irradiance over time and/or the volume of water to be treated. The influence of some inorganic ions typically occurring in wastewaters in TiO₂-assisted photocatalytic efficiency was also determined in a lab-scale CPC photoreactor equipped with a solar radiation simulator. Moreover, the formation of different reactive species, hydroxyl radical, and singlet oxygen were probed using selective scavengers.

Materials and methods

Reagents

Amoxicillin (MW: 365.4, CAS#26787-78-0, molecular structure and UV absorbance spectrum in Fig. 1) was purchased from Sigma. Titanium dioxide was Degussa P-25 (80 % anatase and 20 % rutile). Acetonitrile, methanol, and oxalic acid dihydrate were obtained from Merck. Ultrapure and pure water necessary for analysis were obtained using a millipore system (Direct-Q model) and reverse osmosis system (Panice®), respectively. NaCl, MgSO₄·7H₂O, NaHCO₃, KNO₃, NH₄Cl, K₃PO₄·3H₂O, D-mannitol, and NaN₃ were all analytical grade.

Pilot plant and lab-scale photoreactors description

The solar photolytic and photocatalytic experiments were carried out in a CPC pilot plant. A schematic representation of the pilot plant can be seen in Fig. 2a. The solar collector consists of a CPC unit (0.91 m²) of four borosilicate (Duran) tubes (cutoff, 280 nm; internal diameter, 46.4 mm;

length, 1,500 mm; and width, 1.8 mm) connected in series by polypropylene junctions, with their CPC mirrors in electropolished anodized aluminum, supported by an aluminum structure, oriented to south and tilted 41° (local latitude). The pilot plant has also two recirculation tanks (10 and 20 L), two recirculation pumps (flow rate=20 L min⁻¹), two flow rate meters, five polypropylene valves, and an electric board for process control. The pilot plant can be operated in two ways: using the total CPCs area (0.91 m²) or using 0.455 m² of CPCs area individually, giving the possibility of performing two different experiments at the same time and under the same solar radiation conditions. The intensity of solar UV radiation is measured by a global UV radiometer (ACADUS 85-PLS) mounted on the pilot plant with the same inclination, which provides data in terms of incident \overline{W}_{UV} per square meter.

Equation 1 allows the calculation of the amount of accumulated UV energy ($Q_{UV,n}$, in kilojoules per liter) received on any surface in the same position with regard to the sun, per unit of volume of water inside the reactor, in the time interval Δt :

$$Q_{UV,n} = Q_{UV,n-1} + \Delta t_n \overline{UV}_{G,n} \frac{A_r}{1,000 \times V_t}; \quad \Delta t_n = t_n - t_{n-1} \quad (1)$$

where t_n is the experimental time of each sample, V_t the total reactor volume (in liter), A_r the illuminated collector surface area (in square meter), and $UV_{G;n}$ is the average solar ultra-violet radiation (in Watts per square meter) measured during the period Δt_n (in seconds).

The set of experiments testing the influence of inorganic ions on the AMX photocatalytic degradation and the formation of different reactive species, hydroxyl radical, and singlet oxygen, using selective scavengers were carried out in a lab- scale photoreactor with a sunlight simulator. Figure 2b presents a scheme of the photocatalytic system which comprises:

- (1) a solar radiation simulator (ATLAS, model SUNTEST XLS+) with 1,100 cm² of exposition area, a 1,700-W air-cooled xenon arc lamp, a daylight filter, and quartz filter with infrared coating;
- (2) a compound parabolic collector with 0.023 m² of illuminated area with electropolished anodized aluminum reflectors and borosilicate (Duran) tube (cutoff, 280 nm; internal diameter, 46.4 mm; length, 160 mm; and thickness, 1.8 mm);
- (3) one glass vessel (capacity of 1.5 L) with a cooling jacket coupled to a refrigerated thermostatic bath (Lab. Companion, model RW-0525G) to ensure a constant temperature during the experiment;
- (4) a magnetic stirrer (Velp Scientifica, model ARE) to ensure complete homogenization of the solution inside the glass vessel;
- (5) one peristaltic pump (Ismatec, model Ecoline VC-380 II, with a flow rate of 0.63 L min⁻¹) to promote the water recirculation between the CPC and the glass vessel; and
- (6) pH and temperature meter (VWR symphony, SB90M5). All the systems are connected using Teflon tubing. The intensity of the UV radiation was measured by a broadband UV radiometer (Kipp & Zonen B.V., model CUV5), which was placed in the interior of the sunlight simulator at the same level as the photoreactor center. The radiometer was plugged into a handheld display unit (Kipp & Zonen B.V., model Meteor) to record the incident irradiance (in Watts per square meter).

Experimental procedures

Solar pilot plant

Solar photolytic and photocatalytic experiments were carried out using 20 mg L^{-1} of AMX, and both antibiotic and DOC concentrations were followed. For these experiments, 15 L (illuminated volume (V_i)=5.1 L, $V_i/V_t=0.34$; illuminated time (t_i)=0.25 min, dark time (t_{dark})=0.50 min; $ACPC=0.455 \text{ m}^2$) of the solution to be tested were added to the recirculation tank of the solar CPC unit and homogenized by turbulent recirculation for 30 min in darkness. After pH adjustment to a value around 7.5 with 14 M NaOH (few drops), a sample was taken. This pH value was chosen given that several authors have already reported the influence of pH on TiO_2 -mediated photocatalytic degradation of AMX and found minimal influence in the near-neutral pH range (Elmolla and Chaudhuri 2010b; Klauson et al. 2010; Dimitrakopoulou et al. 2012). The suspended catalyst load for photocatalysis was 0.5 g L^{-1} of TiO_2 , which is able to absorb all solar UV photons considering an internal photoreactor tube diameter of 46.4 mm (Colina-Márquez et al. 2010). Thirty minutes after TiO_2 addition, another sample was taken to determine the AMX adsorption onto the catalyst surface (which was found out to be less than 2 % in average), and then the CPCs were uncovered in order to begin the photocatalytic experiments. Throughout the reaction, samples were taken at predefined times to monitor the photodegradation process. All samples were prefiltered through $0.45 \text{ }\mu\text{m}$ nylon membrane filters (VWR) before analysis and both temperature and pH were measured using a pH meter HANNA HI 4522. To assess AMX photolysis, the same methodology was used but in the absence of TiO_2 . In the photocatalytic experiment using an initial antibiotic concentration of 40 mg L^{-1} , antibacterial activity and mineralization efficiency calculated from DOC, inorganic ions concentration, and low molecular weight carboxylate anions concentration present in the solution, were also assessed. In this case, a volume of 20 L of the solution was used following the same procedure. A higher concentration of antibiotic solution was used in order to have enough resolution in low molecular weight carboxylate anions and inorganic ions analysis.

Lab-scale photoreactor

A similar procedure to study the influence of common occurring ions (Cl^- , SO_4^{2-} , NO_3^- , NH_4^+ , PO_4^{3-} ; 1 g L^{-1} and HCO_3^- ; 0.1 g L^{-1}) in various types of wastewaters (Boaventura et al. 1997; Vilar et al. 2009; Sousa et al. 2012) and the formation of different reactive species, hydroxyl radical, and singlet oxygen, using selective scavengers (50 mM of D-mannitol and 10 mM NaN_3 , respectively; Hirakawa et al. 2004; Raja et al. 2005), was carried out in the lab-scale apparatus. The recirculation glass vessel of the lab-scale prototype was filled with 1 L of 20 mg L^{-1}

AMX solution, which was pumped to the CPC unit ($V_i=270$ mL, $V_i/V_t=0.27$, $t_i=0.43$ min, $t_{\text{dark}}=1.16$ min, $A_{\text{CPC}}=0.023$ m²) and homogenized by recirculation in the closed system during 15 min in the dark.

The temperature set-point of the refrigerated thermostatic bath was controlled to keep the solution at a temperature of 25 °C. After pH adjustment (7.5) and temperature stabilization, the corresponding salt mass to achieve the desired concentration of each ion or scavenger to be studied was added to the solution. After 15 min, a sample was taken before the catalyst addition step (0.5 g L⁻¹ TiO₂). The SUNTEST was turned on and the radiation intensity (I) was set to 500 WUVm⁻², which is equivalent to 44 WUVm⁻² measured in the wavelength range from 280 to 400 nm. Over the reactions, samples were taken at predefined times and prefiltered through 0.45 µm nylon VWR membrane filters before analysis to assess the photodegradation process.

Analytical procedures

AMX concentration was measured by a Hitachi ELITE LaChrom HPLC (Merck-Hitach, Tokyo, Japan), equipped with a L-2130 pump, a L-2200 autosampler, a L-2300 column oven, and a L-2455 DAD. The reverse-phase column Purospher® RP-18e 125-4 (5 µm; Merck) was operated at room temperature (25 °C). The eluent was delivered at a flow rate of 0.8 mL min⁻¹ in gradient mode using acetonitrile (mobile phase A), methanol (mobile phase B), and 0.01 M oxalic acid aqueous solution (mobile phase C, previously filtered by 0.20 µm nylon filter and degassed). Pump program for AMX gradient run was as follows: $t=0$ min (10:5:85), $t=5$ min (20:5:75), $t=7$ min (10:5:85), and $t=14$ min (10:5:80) for acetonitrile/methanol/oxalic acid, respectively. Injection volume was 20 µL and the wavelength of the UV absorbance detector was set at 231 nm. DOC content was determined in a TC-TOC-TN analyzer equipped with an ASI-V autosampler (Shimadzu, model TOC-VCSN) and provided with a NDIR detector, calibrated with standard solutions of potassium hydrogen phthalate (total carbon) and a mixture of sodium hydrogen carbonate/carbonate (inorganic carbon). Total nitrogen was measured in the same TC-TOC-TN analyzer coupled with a TNM-1 unit (Shimadzu, model TOC-VCSN) calibrated with standard solutions of potassium nitrate, through thermal decomposition and NO detection by chemiluminescence method.

Sulfate, nitrite, nitrate, and low molecular weight carboxylate anions (acetate, propionate, formate, pyruvate, valerate, malonate, maleate, oxalate, and citrate) were monitored by ion chromatography (Dionex ICS-2100; column, AS 11-HC (4×250 mm); suppressor, ASRS®300 (4 mm)). Ammonium was also monitored by ion chromatography (Dionex DX-120; column, CS12A (4 × 250 mm); suppressor, CSRS®300 (4 mm)). Isocratic elution was performed using 30 mM NaOH/20 mM methane sulfonic acid at a flow rate of 1.5 and 1.0 mL min⁻¹ for anions and cations analyses, respectively. The gradient program used for the quantification of low molecular weight carboxylate anions comprised a pre-run for 8 min with 1 mM NaOH, 20 min with 30 mM NaOH, and 10 min

with 60 mM NaOH, at a flow rate of 1.5 mL min^{-1} , using an eluent generator cartridge (Dionex, RFICTM).

The antimicrobial activity was assessed by the biomass yield of strains *Escherichia coli* DSM 1103 and *Staphylococcus aureus* DSM 1104 grown for 24 h in filter-sterilized phototreated samples supplemented with 2 g L^{-1} yeast extract, measured by changes in optical density ($\lambda=610 \text{ nm}$) and normalized by that of a positive control grown in mineral medium B (Barreiros et al. 2003) supplemented with the same concentration of yeast extract. All the assays were performed in triplicate.

A pseudo-first-order mathematical model was fitted to the experimental data obtained from the kinetic studies by a nonlinear regression method using Fig.P for Windows from Fig.P Software Incorporated. The model parameters were obtained by minimizing the sum of the squared deviations between experimental and predicted values. Model goodness was evaluated through the calculation of relative standard deviations (σ_i), regression coefficients (R^2) and residual variances (S^2).

Results and discussion

Pilot-scale AMX photolysis and photocatalysis

To rule out the influence of solar photolysis on the degradation of AMX, an experiment with 20 mg L^{-1} in aqueous solution was carried out in the absence of TiO_2 . Figure 3 shows that direct photolysis was unable to considerably attack the molecules of the antibiotic and did not mineralize them in the given period of solar exposure (irradiation time (t_{ir})=215 min). This can be explained by the fact that the absorption of UV radiation, from the range of solar UV radiation that enters the reactor, by the AMX molecule is negligible, as seen by the very low overlapping spectra in Fig. 1, as highlighted in Rizzo et al. (2012). Xu et al. (2011) reported that direct photolysis in a solar simulator accounted for 6–21 % of AMX loss in simulated natural waters, albeit for significantly higher exposure times (40 h) than the ones performed in this work (5 h of exposure in average). The solar photocatalytic degradation of AMX was studied for a TiO_2 load of 0.5 g L^{-1} and $\text{pH}=7.5$. After 3.1 kJuv of accumulated UV energy per liter of solution in the system (Fig. 3; $t_{ir}=60 \text{ min}$), the AMX concentration was below the respective detection limit (0.11 mg L^{-1}). At the same point, DOC suffered a steep reduction down to 39 % of its original value (61 % of mineralization). After an accumulation of 10 kJUV L^{-1} ($t_{ir}=204 \text{ min}$), this percentage was slowly lowered down to 27 %, showing that the AMX intermediary by-products remaining in solution were more difficult to mineralize. Our results agree with Klauson et al. (2010), who reported a 80 % conversion of 20 mg L^{-1} AMX (initial $\text{pH} 6.0$) using 1 g L^{-1} of TiO_2 after 2

h of exposure to solar radiation in an evaporation dish batch reactor.

The kinetic results showed that the TiO₂-assisted photocatalytic process follows a pseudo-first-order reaction, and the rate constant for AMX was calculated as $0.80 \pm 0.02 \text{ L kJ}_{\text{UV}}^{-1}$, while the initial reaction rate (r_0) was $16.0 \pm 0.3 \text{ mg kJ}_{\text{UV}}^{-1}$ (Table 1). In a previous work (Pereira et al. 2013), under the same experimental conditions, pseudo-first-order kinetic rate constants five and two times higher were obtained for oxytetracycline (OTC) and oxolinic acid (OXA), respectively. It must be underlined that despite the difference between the molar concentrations used ($0.087 \text{ mmol OTC L}^{-1}$, $0.109 \text{ mmol AMX L}^{-1}$, and $0.153 \text{ mmol OXA L}^{-1}$) was not that high, the studied antibiotics present notable differences in terms of structure and functional groups, which may influence their adsorption properties onto the photocatalyst surface (Figueroa-Diva et al. 2010) and the susceptibility to solar UV radiation absorption and attack of the reactive oxidant species.

Evaluation of the AMX mineralization

To better understand the effectiveness of the solar photocatalytic degradation of AMX, an experiment using an antibiotic concentration of 40 mg L^{-1} was carried out under the same initial conditions. As shown in Fig. 4, AMX was almost fully degraded (residual concentration = 3.1 mg L^{-1}) after $4.6 \text{ kJ}_{\text{UV}}$ of accumulated UV energy per liter of solution ($t_{\text{IR}} = 110 \text{ min}$), achieving a mineralization of 44 %. Of the organic carbon in the solution (according to the carboxylic acids analyzed), 21 % is attributed to low molecular weight carboxylate anions, mainly formic, propionic, and maleic acids. However, most of the other organic intermediates still contained sulfur and nitrogen, since only 17 % of the total nitrogen in solution was detected in the form of ammonium ($[\text{NAMX}]_t = 4.6 \text{ mg L}^{-1}$) and only 69 % of the stoichiometric quantity of sulfate ($[\text{SAMX}]_t = 1.75 \text{ mg L}^{-1}$) was already released.

The TiO₂ solar photocatalysis was able to reduce the remaining DOC content to 29 % of the original value after $11.7 \text{ kJ}_{\text{UV}} \text{ L}^{-1}$ sunlight exposure ($t_{\text{I}} = 351 \text{ min}$). Seventy percent of the residual DOC content was in the form of low molecular weight carboxylate anions, mainly propionic and maleic acids, which is consistent with the decrease in the initial pH level down to around 6.40 in the same phototreatment period. The amount of sulfate detected at the end of the reaction corresponds to the stoichiometric conversion of sulfur contained in AMX to sulfate ion showing that its complete mineralization occurred and that sulfur was not present in the remaining organic by-products. On the other hand, the ongoing degradation of nitrogenated by-products was less effective during the same period as only 30 % of the initial nitrogen was converted to ammonium by the end of the process. No losses of nitrogen have been observed from the monitoring of total nitrogen; therefore, the enduring nitrogen atoms are not present in nitrogenated organics adsorbed onto the surface of the catalyst. Lower levels of mineralization of sulfur and nitrogen contained in AMX have been reported by Klauson et al. (2010), releasing 14 and 1.4 %, respectively.

respectively. Elmolla and Chaudhuri (2010b) reported the need of long irradiation times for the mineralization of sulfur contained in a mixture of amoxicillin and two other β -lactam antibiotics in aqueous solution under UV-A/TiO₂/H₂O₂ photocatalysis.

Minimum inhibitory concentrations (MICs) are defined as the lowest concentration required to inhibit the visible growth of a microorganism in contrast to a positive control (Carson et al. 1995) and are used by diagnostic laboratories mainly to confirm resistance (Miller et al. 2005). For the enterobacterial strain tested, AMX antibacterial activity with an accumulation of 4.6 kJUVL⁻¹ (t_{ir} =110 min) in the system was found to be considerably reduced when growth was compared to the control (Fig. 5). Antibiotic concentration in this point, [AMX]=3.1 mg L⁻¹, was slightly below the value which Andrews (2001) reported to be sufficient to inhibit *E. coli* growth (4 mg L⁻¹). Conversely, at the same point, *S. aureus* growth was still inconsequential, as the defined MIC value of 0.25 mg L⁻¹, reported in the same study (Andrews 2001), is considerably lower. When a QUV amount of 6.4 kJUVL⁻¹ (t_{ir} =150 min) was reached ([AMX] below the detection limit of the equipment, 0.11 mg L⁻¹), AMX antibacterial activity against *E. coli* was completely relieved, and some *S. aureus* growth occurred, though half of that of the positive control. In a UV-A/TiO₂ photocatalysis experiment with 30 mg L⁻¹ of AMX, Dimitrakopoulou et al. (2012) reported that antibacterial activity against two different bacterial strains belonging to the Enterobacteriaceae family, with broader MIC values than the strains used in this study, was inactivated when AMX concentration dropped below 25 mg L⁻¹. However, for a concentration below 5 mg L⁻¹, an enterococci bacterial strain studied by the same authors showed to be affected, especially by AMX intermediary by-products. According to the reaction pathways proposed by Klauson et al. (2010), some of the AMX photocatalytic by-products (identified via UPLC-ESI-MS analysis) still contain an intact β -lactamic ring structure, which accounts for this residual antibacterial activity. Consequently, in this work, an accumulated UVenergy value of 7.7 kJUVL⁻¹ (t_{ir} =180 min) is suggested to be enough to achieve the complete cleavage of the β -lactamic ring, as the solution no longer presented antibacterial activity against *S. aureus* (Fig. 5), and no longer presents the risk of promoting antibiotic resistance among bacteria in the potential receiving water body.

Some works have reported the adsorption of penicillin antibiotics on non-illuminated iron and TiO₂ nanoparticles and the consequent breakdown of the β -lactamic ring of the original compounds over different pH conditions (Ghauch et al. 2009; Peterson et al. 2012). However, in the photocatalytic experiments performed in this work, no significant loss of AMX was seen in the period of time between the catalyst addition step and the beginning of the irradiation.

The photocatalytic pseudo-first-order kinetic constant for AMX was found to be 0.43±0.01 L kJUV⁻¹, approximately half of the kinetic constant obtained in the first experiment (20 mg L⁻¹ AMX; Table 1). As the initial dark adsorption of AMX onto the photocatalyst surface was

minimal and very similar in both experiments, the calculated initial reaction rate was in this case $18.9 \pm 0.4 \text{ kJ}_{\text{UV}}^{-1}$

Influence of inorganic ions and scavengers

Inorganic ions, such as those present in various types of wastewaters, have been found to inconsistently affect the rates⁴of photocatalytic oxidation of organic pollutants (Abdullah 1990; Ahmed et al. 2010). Figure 6a presents the individual effect of Cl^- , SO_4^{2-} , PO_4^{3-} , NO_3^- and NH_4^+ (1 g L^{-1}), and HCO_3^- (0.1 g L^{-1}) on the photocatalytic ($0.5 \text{ g L}^{-1} \text{ TiO}_2$) degradation of AMX (20 mg L^{-1}) after an endpoint of 60 min of simulated solar irradiation in the lab-scale photoreactor. Guillard et al. (2005) have shown that the decrease in efficiency of TiO_2 photocatalysis in the presence of inorganic ions at neutral pH conditions is mainly caused by the formation of an inorganic layer at the catalyst surface, inhibiting the contaminant adsorption. Under the tested pH value, and according to Fig. 1b, c, the AMX species in solution may present overall neutral (48.5 % as H_2AMX) or negative charges (49.7 % as HAMX^-), and the surface of TiO_2 particles is neutral and negatively charged (76 % as $-\text{TiOH}$ and 24 % as $-\text{TiO}^-$; $\text{pH} > \text{pHPZC}$, pH of point of zero charge = 6.7; Fernández- Ibáñez et al. 2003; Malato et al. 2009). According to Dimitrakopoulou et al. (2012), this does not favor an electro- static attraction between AMX and TiO_2 , and leads to the minimal amount of antibiotic adsorption in the dark, as it can be seen in Fig. 6a. Consequently, the aforementioned effect of the presence of most inorganic ions did not substantially affect the AMX photocatalytic kinetic rates (Table 1). The only considerable exception is the case of PO_4^{3-} , whose presence not only promoted the initial dark adsorption of AMX onto the catalyst surface, but consequently enhanced the oxidation rate of AMX compared to its absence (Fig. 6a). Chen et al. (2003) have reported a similar phenomenon of increased adsorption of certain dye-constituent aromatics on the surface of TiO_2 in the presence of phosphate anions. The negatively charged phosphate anions strongly adsorbed onto the TiO_2 surface may favor not only the adsorption of AMX species bearing a positive (Chen et al. 2003) or neutral (Guillard et al. 2003) charge on the $-\text{NH}_2$ group, but also the formation of free hydroxyl radicals via the enhancement of the separation of the photogenerated hole and electron facilitated by an inner- sphere surface complex, as suggested by Zhao et al. (2008). The same authors thus concluded that phosphate modification accelerates the degradation of pollutants either more prone to hydroxyl radical attack or with weak adsorption on pure TiO_2 particles.

To evaluate the role of reactive species, such as $\cdot\text{OH}$ and singlet oxygen ($^1\text{O}_2$), in the AMX photocatalytic degradation, selective scavengers D-mannitol and sodium azide (NaN_3), respectively, were used. The insignificant photocatalytic degradation of the antibiotic during the phototreatment period in the presence of D-mannitol (Fig. 6b and Table 1), purports the role of $\cdot\text{OH}$ radicals as the major responsible for AMX degradation, which is in agreement with the results presented by Song

et al. (2008). However, according to Fig. 6b, the $^{1}O_2$ reactive species also plays an important role in AMX self-photosensitization under UV/visible solar light, as reported by Zhao et al. (2013).

Solar photocatalytic efficiency index

In the case of AOPs based on free solar radiation, the main capital cost is proportionally related to the area of the collectors. As such, it is suitable to use a figure-of-merit based on the solar collector area recommended by the International Union of Pure and Applied Chemistry (IUPAC) to allow for a direct comparison between the solar energy efficiency of different AOPs, independently of the nature of the used system. Therefore, for a low-pollutant concentration range, the appropriate figure-of-merit is the ACO (Bolton et al. 2001). ACO is the collector area required to reduce the concentration of a contaminant (C) in polluted water in a unit of volume by one order of magnitude in a time ($t_0=1$ h) when the standardized incident solar irradiance (E_S^0) is $1,000 \text{ W m}^{-2}$. The ACO (in square meter per cubic meter order), in batch operation, can be calculated from Eq. 2:

$$A_{CO} = \frac{A_r \cdot \overline{UVG} \cdot t}{E_S^0 \cdot t_0 \cdot V_r \cdot \log\left(\frac{C}{C_0}\right)} \quad (2)$$

where A_r is the illuminated collector surface area (in square meter), UVG is the average solar ultraviolet irradiance (in Watts per square meter, as measured in the 300–400 nm range, the useful UV wavelength range for solar photocatalysis with TiO_2) over the period t of the treatment (in hour), V_r the total reactor volume (in cubic meter), and C and C_0 are the final and initial antibiotic concentrations (in milligram per liter). This figure-of-merit indicates a loss in the system efficiency when ACO values increase, in an inverse proportion. As previously mentioned, CPC geometry has been shown to be highly efficient when applied to solar photocatalytic treatments. This remark has been emphasized by Bandala and Estrada (2007), when they compared the same figure-of-merit using different solar reactors (which use direct and diffuse UV irradiation).

Within this study, for the two different initial antibiotic concentrations, 20 and 40 mg L^{-1} , 0.85h ($UVG = 25.2 \text{ W m}^{-2}$) and 1.65h ($UVG = 32.18 \text{ W m}^{-2}$)h were required to achieve a decrease of the initial AMX concentrations in 1 order of magnitude, resulting in an ACO index of 0.65 to $1.21 \text{ m}^2 \text{ m}^{-3}$ order, respectively. It should be mentioned that the 30 % solar UV irradiance increase between experiments (given that these were performed in different days) was compensated by a decrease of the useful solar exposure time needed to reduce the AMX concentration by an order of magnitude. Therefore, according to the results obtained, there is no substantial conversion efficiency loss in the studied antibiotic concentration range. As expected, a twofold increase of pollutant concentration only doubled the ACO index. A similar system efficiency was obtained by Sousa et al. (2013) in the solar photocatalytic oxidation of the anxiolytic drug lorazepam using the same pilot plant but mediated by only 0.2 g L^{-1} TiO_2 (ACO index = $0.4 \text{ m}^2 \text{ m}^{-3}$ order).

Conclusions

The use of CPC photoreactors for solar UV photons capture was shown to be effective for the TiO_2 -assisted photocatalytic ($[\text{TiO}_2]=0.5 \text{ g L}^{-1}$) degradation of the antibiotic amoxicillin in aqueous solutions at neutral pH conditions (7.5). Solar UV radiation alone was unable to attack the antibiotic molecules during the same phototreatment period. The TiO_2 solar photocatalysis was able to reduce the antibiotic concentration from 40 to 3.1 mg L^{-1} after $4.6 \text{ kJ}_{\text{UV}}$ of UV accumulated energy per liter of solution, leading to a considerable reduction of the antibacterial activity. At the end of the phototreatment period ($11.7 \text{ kJ}_{\text{UV}}\text{L}^{-1}$ of UV energy accumulated in the system), 71 % mineralization was achieved, being 70 % of the residual DOC content in the form of low molecular weight carboxylate anions, mainly propionic and maleic acids. Even though the amount of sulfate detected at the end of the reaction corresponds to the stoichiometric conversion of sulfur contained in AMX, only 30 % of the initial nitrogen was converted to ammonium, showing that the mineralization of nitrogenated by-products was less effective during the phototreatment period. Although the AMX degradation was mainly attributed to hydroxyl radicals, singlet oxygen also plays an important role in AMX self-photosensitization under UV/visible solar light. Screenings of individual inorganic ions effects have shown that the presence of phosphates at the studied pH level enhance AMX photocatalytic oxidation, while the presence of other inorganic ions (Cl^- , SO_4^{2-} , NO_3^- , NH_4^+ , and HCO_3^-) did not considerably alter the reaction rate. The results obtained build on the potential for developing future treatments for wastewaters of various origins containing high concentrations of AMX with relatively short periods of solar irradiance, allowing their subsequent safe discharge due to the elimination of the risk of antibiotic resistance promotion.

Acknowledgments This work is partially supported by project PEst-C/EQB/LA0020/2011, financed by FEDER through COMPETE-Programa Operacional Factores de Competitividade, by Fundação para a Ciência e a Tecnologia (FCT) and by the project PTDC/AAC-AMB/113091/2009. João H. O. S. Pereira acknowledges his doctoral fellowship (SFRH/BD/ 62277/2009) supported by Fundação para a Ciência e a Tecnologia (FCT). Vítor J. P. Vilar acknowledges Ciência 2008 Program.

References

- Abdullah M (1990) Effects of common inorganic anions on rates of photocatalytic oxidation of organic carbon over illuminated titanium dioxide. *J Phys Chem* 94:6820–6825
- Ahmed S, Rasul MG, Martens WN, Brown R, Hashib MA (2010) Heterogeneous photocatalytic degradation of phenols in waste-water: a review on current status and developments. *Desalination* 261:3–18
- Andreozzi R, Caprio V, Ciniglia C, De Champdoré M, Lo Giudice R, Marotta R, Zuccato E (2004) Antibiotics in the environment: occurrence in Italian STPs, fate, and preliminary assessment on algal toxicity of amoxicillin. *Environ Sci Technol* 38:6832–6838
- Andreozzi R, Canterino M, Marotta R, Paxeus N (2005) Antibiotic removal from wastewaters: the ozonation of amoxicillin. *J Hazard Mater* 122:243–250
- Andrews JM (2001) Determination of minimum inhibitory concentrations. *J Antimicrob Chemother* 48:5–16

- Bandala ER, Estrada C (2007) Comparison of solar collection geometries for application to photocatalytic degradation of organic contaminants. *J Solar Energy Eng Trans ASME* 129:22–26
- Barreiros L, Nogales B, Manaia CM, Silva Ferreira AC, Pieper DH, Reis MA, Nunes OC (2003) A novel pathway for mineralization of the thiocarbamate herbicide molinate by a defined bacterial mixed culture. *Environ Microbiol* 5:944–953
- Boaventura R, Pedro AM, Coimbra J, Lencastre E (1997) Trout farm effluents: characterization and impact on the receiving streams. *Environ Pollut* 95:379–387
- Bolton JR, Bircher KG, Tumas W, Tolman CA (2001) Figures-of-merit for the technical development and application of advanced oxidation technologies for both electric- and solar-driven systems. *Pure Appl Chem* 73:627–637
- Carson CF, Hammer KA, Riley TV (1995) Broth micro-dilution method for determining the susceptibility of *Escherichia coli* and *Staphylococcus aureus* to the essential oil of *Melaleuca alternifolia* (tea tree oil). *Microbios* 82:181–185
- Chen F, Zhao J, Hidaka H (2003) Adsorption factor and photocatalytic degradation of dye-constituent aromatics on the surface of TiO₂ in the presence of phosphate anions. *Res Chem Intermed* 29:733–748
- Colina-Márquez J, MacHuca-Martínez F, Puma GL (2010) Radiation absorption and optimization of solar photocatalytic reactors for environmental applications. *Environ Sci Technol* 44:5112–5120
- Dimitrakopoulou D, Rethemiotaki I, Frontistis Z, Xekoukoulotakis NP, Venieri D, Mantzavinos D (2012) Degradation, mineralization and antibiotic inactivation of amoxicillin by UV-A/TiO₂ photocatalysis. *J Environ Manage* 98:168–174
- Elmolla ES, Chaudhuri M (2009) Degradation of the antibiotics amoxicillin, ampicillin and cloxacillin in aqueous solution by the photo-Fenton process. *J Hazard Mater* 172:1476–1481
- Elmolla ES, Chaudhuri M (2010a) Degradation of amoxicillin, ampicillin and cloxacillin antibiotics in aqueous solution by the UV/ZnO photocatalytic process. *J Hazard Mater* 173:445–449
- Elmolla ES, Chaudhuri M (2010b) Photocatalytic degradation of amoxicillin, ampicillin and cloxacillin antibiotics in aqueous solution using UV/TiO₂ and UV/H₂O₂/TiO₂ photocatalysis. *Desalination* 252:46–52
- Elmolla ES, Chaudhuri M (2010c) Comparison of different advanced oxidation processes for treatment of antibiotic aqueous solution. *Desalination* 256:43–47
- Elmolla ES, Chaudhuri M (2011) The feasibility of using combined TiO₂ photocatalysis-SBR process for antibiotic wastewater treatment. *Desalination* 272:218–224
- Escher BI, Baumgartner R, Koller M, Treyer K, Lienert J, McArdell CS (2011) Environmental toxicology and risk assessment of pharmaceuticals from hospital wastewater. *Water Res* 45:75–92
- Fernández P, Blanco J, Sichel C, Malato S (2005) Water disinfection by solar photocatalysis using compound parabolic collectors. *Catal Today* 101:345–352
- Fernández-Ibáñez P, Blanco J, Malato S, De Las Nieves FJ (2003) Application of the colloidal stability of TiO₂ particles for recovery and reuse in solar photocatalysis. *Water Res* 37:3180–3188
- Figueroa-Diva RA, Vasudevan D, MacKay AA (2010) Trends in soil sorption coefficients within common antimicrobial families. *Chemosphere* 79:786–793

Ghauch A, Tuqan A, Assi HA (2009) Antibiotic removal from water: elimination of amoxicillin and ampicillin by microscale and nano- scale iron particles. *Environ Pollut* 157:1626–1635

González O, Sans C, Esplugas S, Malato S (2009) Application of solar advanced oxidation processes to the degradation of the antibiotic sulfamethoxazole. *Photochem Photobiol Sci* 8:1032–1039

Guillard C, Lachheb H, Houas A, Ksibi M, Elaloui E, Herrmann JM (2003) Influence of chemical structure of dyes, of pH and of inorganic salts on their photocatalytic degradation by TiO₂ comparison of the efficiency of powder and supported TiO₂. *J Photochem Photobiol A Chem* 158:27–36

Guillard C, Puzenat E, Lachheb H, Houas A, Herrmann JM (2005) Why inorganic salts decrease the TiO₂ photocatalytic efficiency. *Int J Photoenergy* 7:1–9

Hirakawa K, Mori M, Yoshida M, Oikawa S, Kawanishi S (2004) Photo- irradiated titanium dioxide catalyzes site specific DNA damage via generation of hydrogen peroxide. *Free Radic Res* 38:439–447

Hirsch R, Ternes T, Haberer K, Kratz KL (1999) Occurrence of antibiotics in the aquatic environment. *Sci Total Environ* 225:109–118

Homem V, Santos L (2011) Degradation and removal methods of antibiotics from aqueous matrices—a review. *J Environ Manage* 92: 2304–2347

Jones OAH, Voulvoulis N, Lester JN (2005) Human pharmaceuticals in wastewater treatment processes. *Crit Rev Environ Sci Technol* 35: 401–427

Kasprzyk-Hordern B, Dinsdale RM, Guwy AJ (2008) The occurrence of pharmaceuticals, personal care products, endocrine disruptors and illicit drugs in surface water in South Wales. *U K Water Res* 42:3498–3518

Kim S, Aga DS (2007) Potential ecological and human health impacts of antibiotics and antibiotic-resistant bacteria from wastewater treatment plants. *J Toxicol Environ Health B Crit Rev* 10:559–573

Klauson D, Babkina J, Stepanova K, Krichevskaya M, Preis S (2010) Aqueous photocatalytic oxidation of amoxicillin. *Catal Today* 151:39–45

Lalumera GM, Calamari D, Galli P, Castiglioni S, Crosa G, Fanelli R (2004) Preliminary investigation on the environmental occurrence and effects of antibiotics used in aquaculture in Italy. *Chemosphere* 54:661–668

Längin A, Alexy R, König A, Kümmerer K (2009) Deactivation and transformation products in biodegradability testing of β -lactams amoxicillin and piperacillin. *Chemosphere* 75:347–354

Leung HW, Minh TB, Murphy MB, Lam JCW, So MK, Martin M, Lam PKS, Richardson BJ (2012) Distribution, fate and risk assessment of antibiotics in sewage treatment plants in Hong Kong, South China. *Environ Int* 42:1–9

Malato S, Blanco J, Vidal A, Richter C (2002) Photocatalysis with solar energy at a pilot-plant scale: an overview. *Appl Catal B Environ* 37:1–15

Malato S, Fernández-Ibáñez P, Maldonado MI, Blanco J, Gernjak W (2009) Decontamination and disinfection of water by solar photocatalysis: recent overview and trends. *Catal Today* 147:1–59

Martinez JL (2009) Environmental pollution by antibiotics and by anti- biotic resistance

determinants. *Environ Pollut* 157:2893–2902 Mavronikola C, Demetriou M, Hapeshi E, Partassides D, Michael C,

Mantzavinos D, Kassinos D (2009) Mineralisation of the antibiotic amoxicillin in pure and surface waters by artificial UVA- and sunlight-induced fenton oxidation. *J Chem Technol Biotechnol* 84: 1211–1217

Michael I, Rizzo L, McArdell CS, Manaia CM, Merlin C, Schwartz T, Dagot C, Fatta-Kassinos D (2013) Urban wastewater treatment plants as hotspots for the release of antibiotics in the environment: a review. *Water Res* 47:957–995

Miller RA, Walker RD, Carson J, Coles M, Coyne R, Dalsgaard I, Giesecker C, Hsu HM, Mathers JJ, Papapetropoulou M, Petty B, Teitzel C, Reimschuessel R (2005) Standardization of a broth microdilution susceptibility testing method to determine minimum inhibitory concentrations of aquatic bacteria. *Dis Aquat Org* 64: 211–222

Mitchell SO, Rodger HD (2011) A review of infectious gill disease in marine salmonid fish. *J Fish Dis* 34:411–432

Noga EJ (2010) *Fish disease: diagnosis and treatment*. Second Edition, Wiley, 536 pp

Oller I, Malato S, Sánchez-Pérez JA (2011) Combination of advanced oxidation processes and biological treatments for wastewater decontamination—a review. *Sci Total Environ* 409:4141–4166

Pereira JHOS, Daniel DB, Reis AC, Nunes OC, Borges MT, Vilar VJP, Boaventura RAR (2013) Insights into solar TiO₂-assisted photocatalytic oxidation of two antibiotics employed in aquatic animal production, oxolinic acid and oxytetracycline. *Sci Total Environ*. doi:10.1016/j.scitotenv.2013.05.098

Peterson JW, Petrasky LJ, Seymour MD, Burkhart RS, Schuiling AB (2012) Adsorption and breakdown of penicillin antibiotic in the presence of titanium oxide nanoparticles in water. *Chemosphere* 87:911–917

Poyatos JM, Muñoz MM, Almecija MC, Torres JC, Hontoria E, Osorio F (2009) Advanced oxidation processes for wastewater treatment: state of the art. *Water Air Soil Pollut* 205(1–4):187–204

Raja P, Bozzi A, Mansilla H, Kiwi J (2005) Evidence for superoxide- radical anion, singlet oxygen and OH-radical intervention during the degradation of the lignin model compound (3-methoxy-4- hydroxyphenylmethylcarbinol). *J Photochem Photobiol A Chem* 169:271–278

Rigos G, Troisi GM (2005) Antibacterial agents in Mediterranean finfish farming: a synopsis of drug pharmacokinetics in important euryhaline fish species and possible environmental implications. *Rev Fish Biol Fish* 15:53–73

Rizzo L, Meric S, Guida M, Kassinos D, Belgiorno V (2009) Heterogenous photocatalytic degradation kinetics and detoxification of an urban wastewater treatment plant effluent contaminated with pharmaceuticals. *Water Res* 43:4070–4078

Rizzo L, Fiorentino A, Anselmo A (2012) Effect of solar radiation on multidrug resistant *E. coli* strains and antibiotic mixture photodegradation in wastewater polluted stream. *Sci Total Environ* 427–428:263–268

Santos LHMLM, Araújo AN, Fachini A, Pena A, Delerue-Matos C, Montenegro MCBSM (2010) Ecotoxicological aspects related to the presence of pharmaceuticals in the aquatic

environment. *J Hazard Mater* 175:45–95

Soares PA, Silva TFCV, Manenti DR, Souza SMAGU, Boaventura RAR, Vilar VJP (2013) Insights into real cotton-textile dyeing wastewater treatment using solar advanced oxidation processes. *Environ Sci Pollut Res*. doi:10.1007/s11356-013-1934-0

Song W, Chen W, Cooper WJ, Greaves J, Miller GE (2008) Free-radical destruction of β -lactam antibiotics in aqueous solution. *J Phys Chem A* 112:7411–7417

Sousa MA, Gonçalves C, Vilar VJP, Boaventura RAR, Alpendurada MF (2012) Suspended TiO₂-assisted photocatalytic degradation of emerging contaminants in a municipal WWTP effluent using a solar pilot plant with CPCs. *Chem Eng J* 198–199:301–309

Sousa MA, Gonçalves C, Pereira JHOS, Vilar VJP, Boaventura RAR, Alpendurada MF (2013) Photolytic and TiO₂-assisted photocatalytic oxidation of the anxiolytic drug lorazepam (Lorenin® pills) under artificial UV light and natural sunlight: a comparative and comprehensive study. *Solar Energy* 87:219–228

Trovó AG, Melo SAS, Nogueira RFP (2008) Photodegradation of the pharmaceuticals amoxicillin, bezafibrate and paracetamol by the photo-Fenton process—application to sewage treatment plant effluent. *J Photochem Photobiol A Chem* 198:215–220

Versporten A et al (2011) European Surveillance of Antimicrobial Consumption (ESAC): outpatient penicillin use in Europe (1997–2009). *J Antimicrob Chemother* 66:vi13–vi23

Vilar VJP, Gomes AIE, Ramos VM, Maldonado MI, Boaventura RAR (2009) Solar photocatalysis of a recalcitrant coloured effluent from a wastewater treatment plant. *Photochem Photobiol Sci* 8:691–698

Watkinson AJ, Murby EJ, Kolpin DW, Costanzo SD (2009) The occurrence of antibiotics in an urban watershed: from wastewater to drinking water. *Sci Total Environ* 407:2711–2723

Xu H, Cooper WJ, Jung J, Song W (2011) Photosensitized degradation of amoxicillin in natural organic matter isolate solutions. *Water Res* 45:632–638

Zhao D, Chen C, Wang Y, Ji H, Ma W, Zang L, Zhao J (2008) Surface modification of TiO₂ by phosphate: effect on photocatalytic activity and mechanism implication. *J Phys Chem C* 112:5993–6001

Zhao C, Pelaez M, Duan X, Deng H, O'Shea K, Fatta-Kassinos D, Dionysiou DD (2013) Role of pH on photolytic and photocatalytic degradation of antibiotic oxytetracycline in aqueous solution under visible/solar light: kinetics and mechanism studies. *Appl Catal B Environ* 134–135:83–92

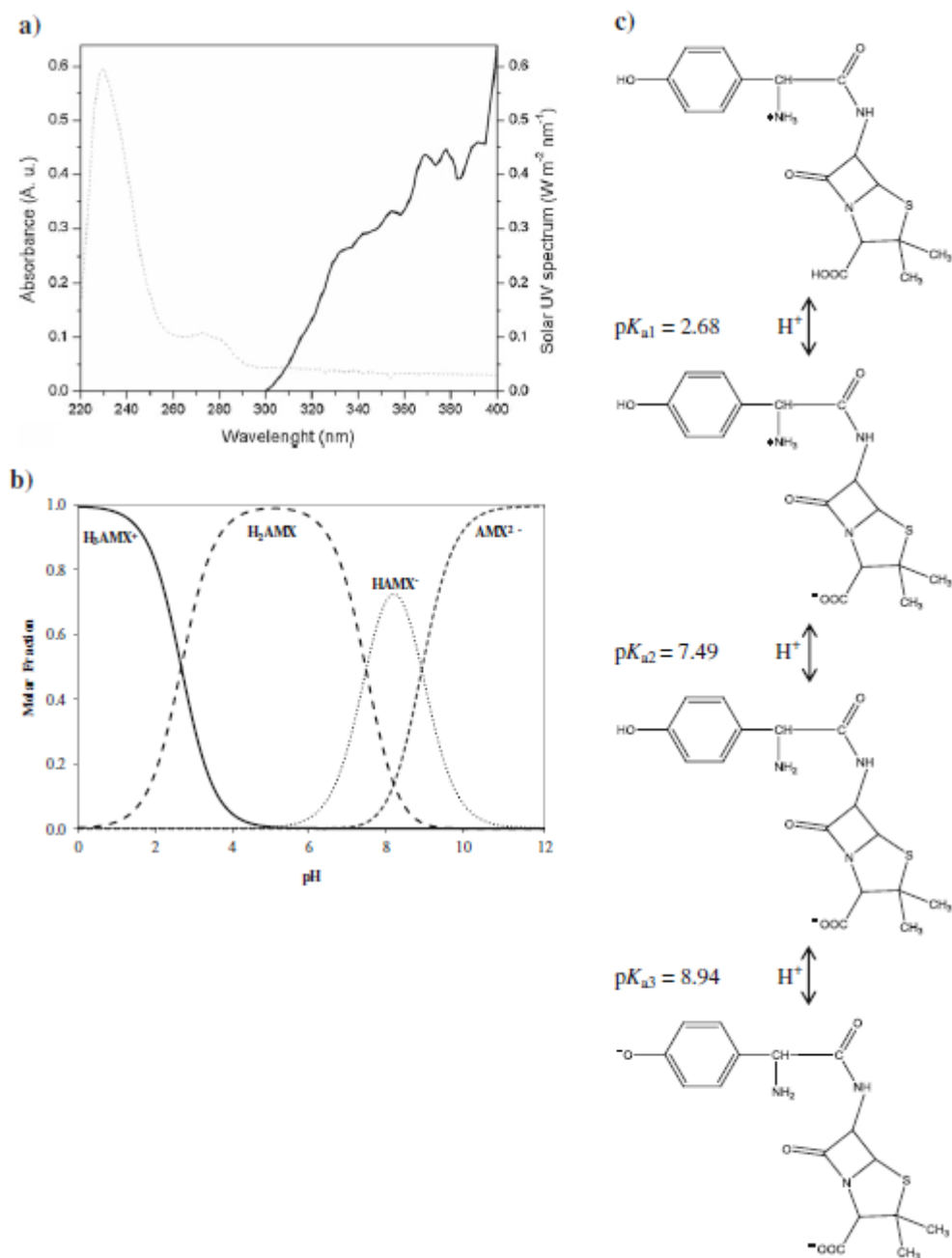


Fig. 1 a Amoxicillin UV absorbance spectrum (*dashed line*) and solar UV spectrum (*solid line*) adapted from Malato et al. (2002). b Antibiotic speciation diagram as a function of pH and c schematics of dissociation equilibrium (pK_a values from Andreozzi et al. (2005). Ionic strength=0.1 M)

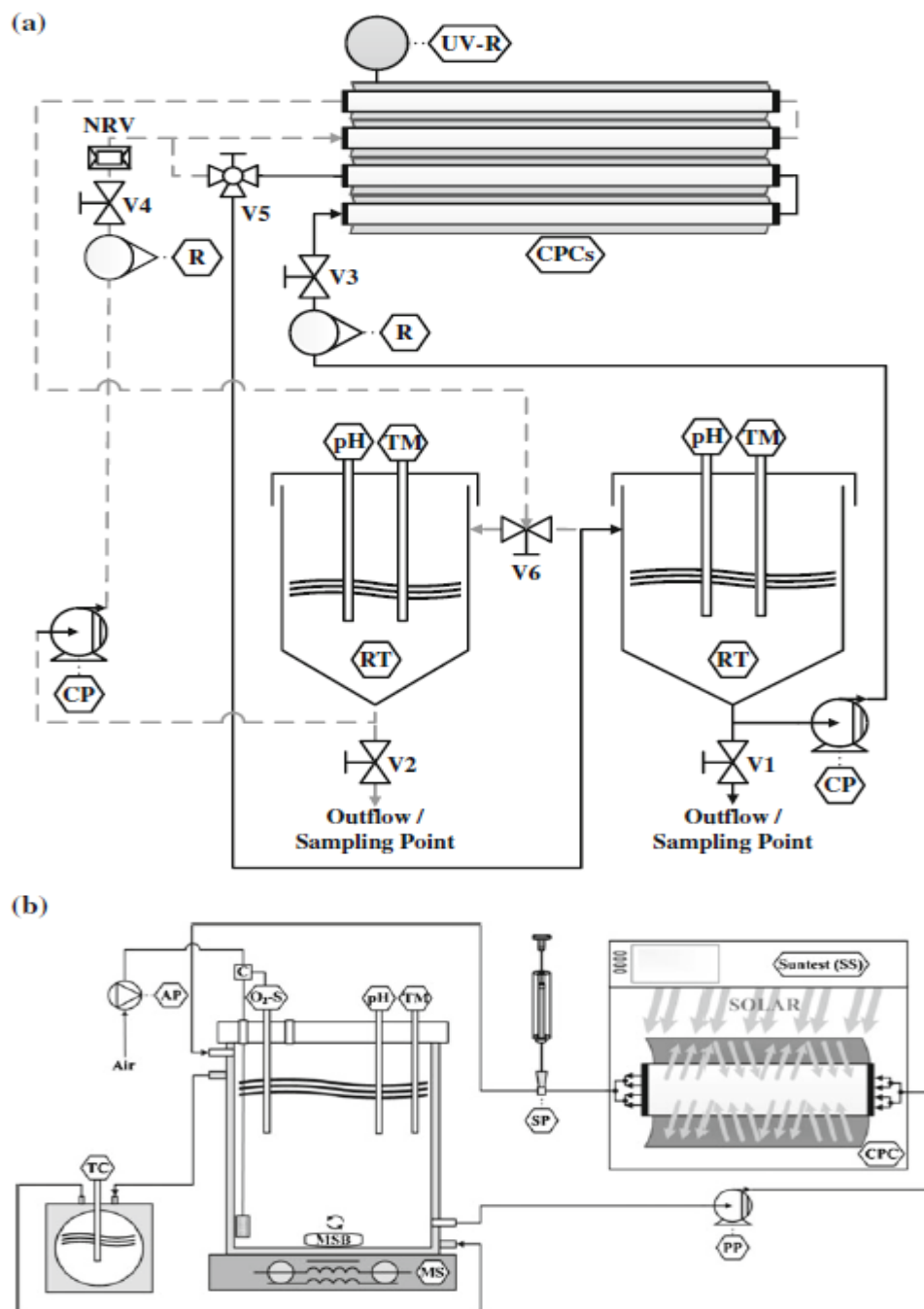


Fig. 2 Flowcharts of the pilot (a) and lab-scale (b) photoreactors. Reprinted (adapted) with permission from Soares et al. (2013). Copyright © 2013, Springer-Verlag Berlin Heidelberg, License Number: 3195790385243. a *TM* temperature meter, *pH* pH meter, *CPCs* compound parabolic collectors, *UV-R* UV radiometer, *RT* recirculation tank, *CP* centrifugal pump, *R* rotameter, *V1* and *V2* recirculation/discharge valves, *V3* and *V4* flow rate control valves, *V5* *CPCs* mode valve, *V6* *RTs* feeding valve; *solid line* main path, *dashed line* alternative path; *NRV* non return valve. b *TC* temperature controller, *PP* peristaltic pump, *AP* air pump, *C* controller, *O₂-S* dissolved oxygen sensor, *pH* pH meter, *TM* temperature meter, *MSB* magnetic stir bar, *MS*

magnetic stirrer, CPC compound parabolic collector, SS Suntest System, SP sampling point

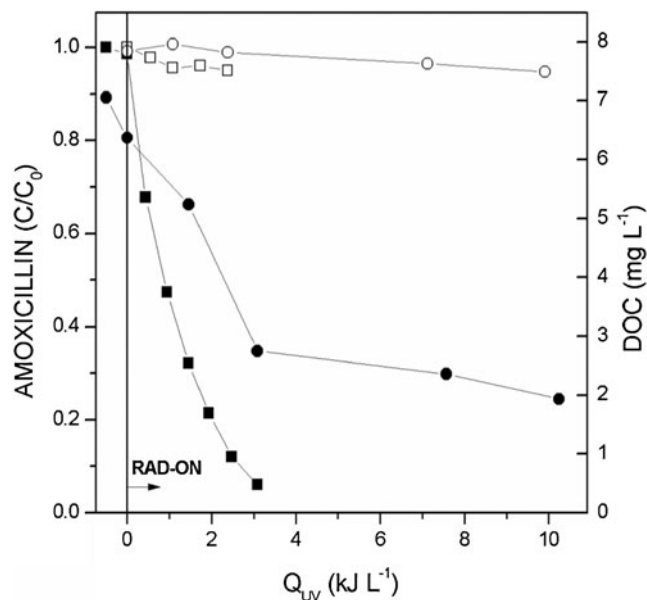


Fig. 3 Solar photolysis (open symbols) and photocatalysis with 0.5 g L^{-1} of TiO_2 (solid symbols) of AMX solutions with 20 mg L^{-1} at $\text{pH}=7.5$: dimensionless AMX concentration (white square, black square) and DOC (white circle, black circle)

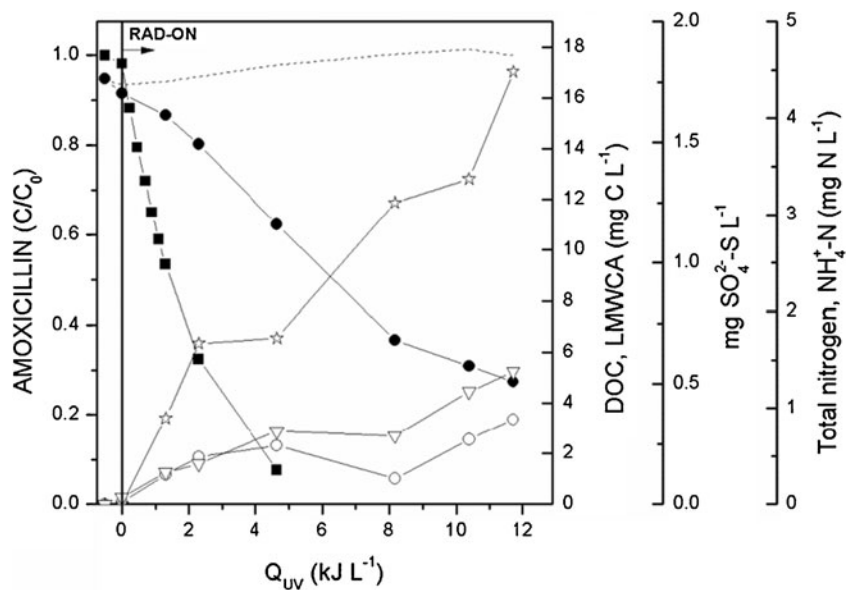


Fig. 4 Solar photocatalysis ($[\text{TiO}_2]=0.5 \text{ g L}^{-1}$) of AMX solution with 40 mg L^{-1} :

dimensionless AMX concentration (*black square*), DOC (*black circle*), sum of low molecular weight carboxylate anions as milligram C per liter (LMWCA, *empty circle*), sulfate as mg SO₄²⁻ S per liter (*star*), total nitrogen (*dashed line*) and ammonium as milligram N per liter (*inverted triangle*)

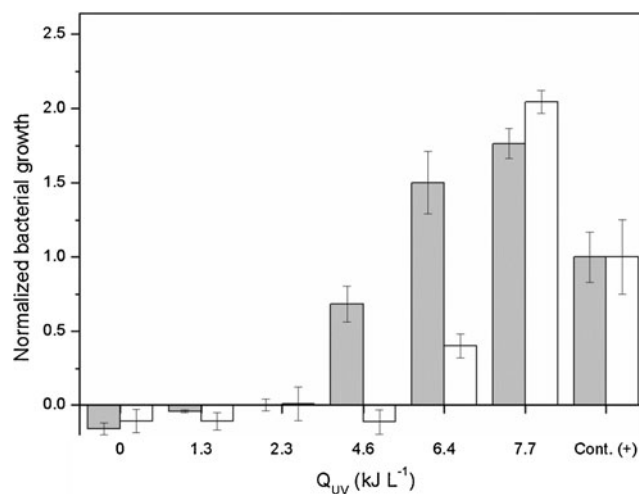


Fig. 5 *Escherichia coli* (gray columns) and *Staphylococcus aureus* (white columns) normalized bacterial growth at different phototreatment times under solar photocatalysis with 0.5 g L⁻¹ of TiO₂ at pH 7.5 ([AMX]₀=40 mg L⁻¹), compared to the respective positive control, Cont. (+)

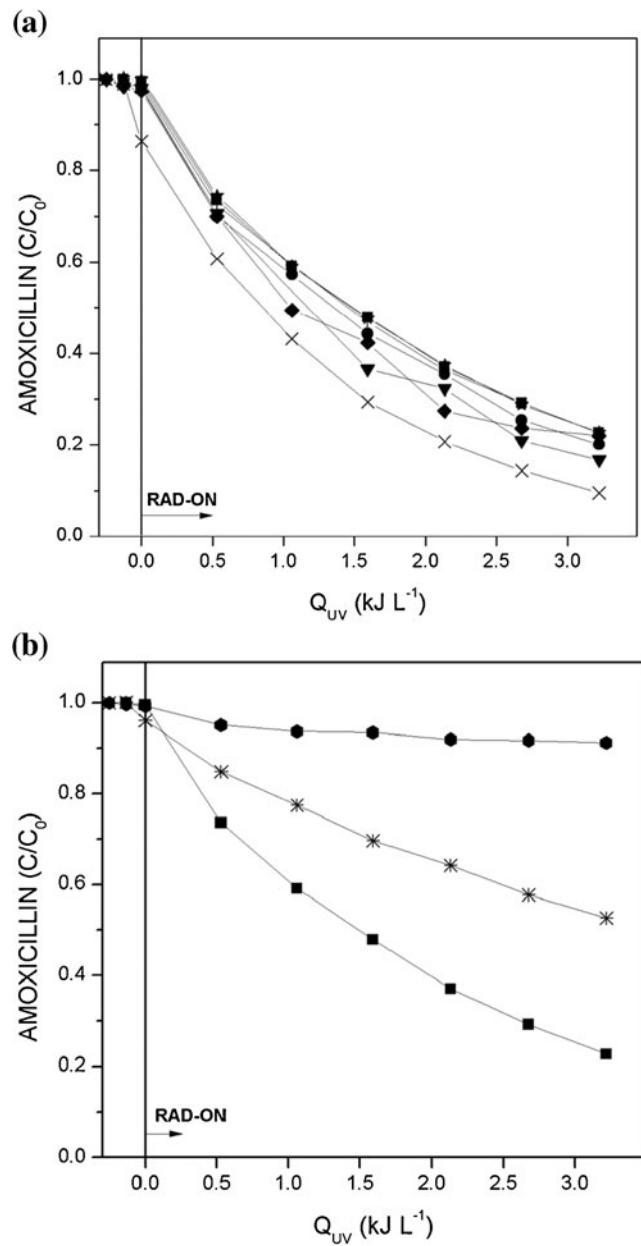


Fig. 6 Removal profiles of 20 mg L⁻¹ of AMX alone (black square) and a in the presence of 1 g L⁻¹ of Cl⁻ (+), SO₄²⁻ (black circle), NO₃⁻ (inverted black triangle), NH₄⁺ (black diamond), PO₄³⁻ (multiplication symbol), 0.1g L⁻¹ HCO₃⁻ (black star) and b in the presence of 10 mM NaN₃ (asterisks) and 50 mM D-mannitol (black hexagon) under simulated solar photocatalysis with 0.5 g L⁻¹ TiO₂ and pH=7.5

Table 1 Pseudo-first-order kinetic constant values for AMX degradation, alone or with (+) inorganic ions and scavengers, under real and simulated solar TiO₂-assisted photocatalytic systems: [TiO₂]=0.5 g L⁻¹; pH=7.5

Experiment	k (L kJ ⁻¹) ^a	r_0 (mg kJ ⁻¹) ^b	R^2	S_R^2 (mg ² L ⁻²)
Solar CPC pilot plant				
20 mg L ⁻¹ AMX	0.80±0.02	16.0±0.3	0.998	0.071
40 mg L ⁻¹ AMX	0.43±0.01	18.9±0.4	0.998	0.331
Lab-scale photoreactor ($I=44$ W m ⁻²)				
20 mg L ⁻¹ AMX	0.47±0.01	8.4±0.2	0.996	0.108
+1.0 g L ⁻¹ Cl ⁻	0.47±0.01	8.3±0.2	0.997	0.119
+1.0 g L ⁻¹ NO ₃ ⁻	0.57±0.02	10.5±0.4	0.996	0.171
+0.1 g L ⁻¹ HCO ₃ ⁻	0.47±0.01	8.9±0.2	0.997	0.095
+1.0 g L ⁻¹ SO ₄ ²⁻	0.5±0.01	8.9±1.8	0.993	0.167
+1.0 g L ⁻¹ NH ₄ ⁺	0.55±0.03	10.3±0.6	0.985	0.513
+1.0 g L ⁻¹ PO ₄ ³⁻	0.669±0.004	10.76±0.06	0.999	0.005
+10 mM NaN ₃	0.193±0.004	3.52±0.01	0.831	0.09
+50 mM D-mannitol	0.032±0.004	0.59±0.07	0.831	0.09

^a Pseudo-first-order kinetic rate

^b Initial reaction rate